Proceedings of the MEDSI 2014 Conference

Melbourne, Australia - October 2014

Design and construction of a 200 TW laser compressor chamber for the Pulsed Laser Center, CLPU facility at Salamanca

Carles Colldelram[1], Alejandro Crisol[1], Juan Hernandez[2], Liudmila Nikitina[1], Marcos Quispe[1], Luis Roso[2]

1. CELLS-ALBA
Carretera BP 1413, de Cerdanyola del Vallès a Sant Cugat del Vallès, Km. 3,3, 08290 Cerdanyola del Vallès (Barcelona), Spain
2. CLPU
BUILDING M5 - SCIENCE PARK - C/ Adaja 8, 37185 - Villamayor (Salamanca), Spain

ccolldelram@cells.es; acrisol@cells.es; jhernandez@clpu.es; lnikitina@cells.es; mquispe@cells.es; roso@clpu.es

Abstract - The Pulsed Laser Center (Centro de Láseres Pulsados, CLPU) is a facility specialized in femtosecond laser pulses with peak powers at Gigawatt, Terawatt and Petawatt levels. The new facility will offer a ladder of laser pulses for different applications: 20TW, 200TW & 1 PW. The facility requires the design and construction of much new optical equipment including the vacuum and mechanical components. One of the critical elements is the compressor and its vacuum system, chamber, and mechanical support. In this article the design of the a new 200 TW laser compressor chamber is presented from the specification requirements up to the final results at site delivery at CLPU Salamanca within the framework collaboration between ALBA – CELLS and CLPU. In this new design all the optical components are mounted on a thick stable breadboard which defines a single flat reference plane for all of them and supported by a robust leveling system based on four columns including a preloaded kinematical mount which reaches stabilities better than 60 nm under vibration behavior. The entire models and FEA calculations accomplish with the specifications and the final measured results match the expected figures achieving a vacuum level below 6•10-7mbar and pumping time less than 10 hours after the chamber enclosure. Parts of this design has been patented, patent application number U201431357.

***Keywords*:** Compressor chamber, Pulsed laser, Vacuum chamber, viewport.

1. Introduction

The Pulsed Laser Center (Centro de Láseres Pulsados, CLPU) is a facility specialized in femtosecond laser pulses with peak powers at Gigawatt, Terawatt and Petawatt levels. The object of the facility is to serve the scientific community and the industry by providing access to state-of-the art high power lasers as well as advice through collaborative research. The facilities are open to national and international users. CLPU is a member of Laserlab Europe and a regional facility of ELI (the European Extreme Light Infrastructure).

The main beam line is a 1 PW (30 Joule / 30 fs) Ti: Sapphire laser system (wavelength centered around 800 nm) operating at 1 Hz repetition rate. This beam line is divided in three phases of increasing power which can be used simultaneously, thus offering a ladder of laser pulses for different applications.

- Phase 1 – 20 TW (600 mJ / 30 fs), 10 Hz

- Phase 2 – 200 TW (6 J / 30 fs), 10 Hz
- Phase 3 – 1 PW (30 J / 30 fs), 1 Hz

Figure 1 shows the Phase 1 – 20TW facility, currently in operation. This laser includes a compressor with a cylindrical chamber that reaches a vacuum level of 5•10-6mbar with a mechanical stability lower than 4 μm displacement under vibration behavior. The vacuum level is reached by means a 150 l/s turbo pump with a primary pump of 75 l/s.

Fig. 1. 200TW laser compressor

2. 200 TW compressor specifications

The specifications for the new facility equipment's are based on the scientific requirements as well as the previous operation experience with the 20 TW compressor chamber. For an optimum performance of the compressor the nominal vacuum level specified is $1 \cdot 10^{-6}$ mbar. Routine use of the compressor system implies to be opened often specially during system commissioning and operation start up. Therefore, it is requested that the pumping time to reach the nominal vacuum level should not exceed 10 hours avoiding long laser operation interruptions. Furthermore, a friendly opening system had to be foreseen in the design.

About the mechanics the optics breadboard reference supports as well as the vacuum chamber support are static systems. The main issue is to ensure a good structural dynamics behavior with minimum vibration displacement amplitudes. Stability values need to be better than 1 μm displacement.

As the previous 20 TW chamber a manual breadboard leveling system is required. The breadboard has to be mounted on kinematical mount including four columns. Resolution must be lower than 30 μrad angularly and 50 μm linearly. The optical base plane should be a flat reference surface on the breadboard top, with a flatness tolerance of 50 μm.

2. 3. Windows

The compressor laser beam path includes separated ports for the input and output of the laser beam. Vacuum and atmospheric environments are isolated by special vacuum windows located on the chamber walls. Figure 2 shows the optics beam path.

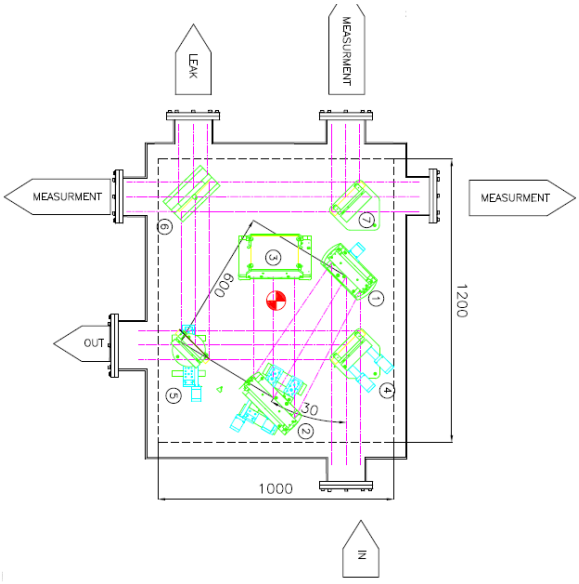

Fig. 2. Compressor optics path

Both ports may be not centered on the vacuum chamber sides, whatever the shape of the chamber would be either cylindrical or rectangular. This means that the deformation of the chamber faces under atmospheric pressure will induce an angular deviation of the window port axis related to the laser beam axis. This misalignment should be lower than 1º.

The vacuum windows of DN200 were proposed to be made of borosilicate glass BK7. Since this glass is not commercially available already mounted on standard vacuum flanges, it was needed a new design for the integration of this glass on a sealed flange. This new concept for the laser viewports should accomplish the maximum acceptable angular deviation. In addition it has to be mounted on a holder which does not introduce any deformation or stress on the borosilicate allowing a free deformation of the material under vacuum pressure.

Table. 1. summarizes the specifications

Characteristic	***Performance***
Vacuum level	$1 \cdot 10^{-6}$ mbar
Pumping time	10 h (up to $5 \cdot 10^{-6}$ mbar)
Mechanical stability	< 1 µm
Breadboard leveling resolution angular	30 µrad
Breadboard leveling resolution linear	50 µm
Breadboard flatness	50 µm
Viewport angular deviation	< 10 mrad

3. Compressor system design

The conceptual design of the chamber, breadboard support and leveling system and the vacuum windows are based on the following principles.

- Rectangular vacuum chamber mounted on a steel frame.

- Stiff and flat optics breadboard
- Stiff preloaded but still adjustable leveling kinematical mount for the breadboard.
- Stiff and stable reference, granite, for the breadboard support decoupled of the vacuum chamber and its fixation.

3. 1. Vacuum chamber design

Although a cylindrical chamber is much more resistant and efficient under vacuum atmospheric pressure a rectangular design is proposed. This solution is justified due to the optical elements space distribution. In this case a cylindrical chamber would be geometrically inefficient needing a large diameter wasting to much unoccupied space.

The main issue of a rectangular vacuum chamber is the high stress. The chamber is a 1800 mm long, 1600 mm width and 700 mm height vacuum vessel which will need thick walls or well distributed reinforcing ribs.

In order to optimize the ribs distribution, material stresses, deformations and viewports axis deviation, some FEA calculations iterations where done. The material used for the chamber is stainless steel AISI-304, Table 2shows this material characterisctics:

Table. 2. AISI-304 Characteristics

Characteristic	***Value***
yield strength	190 MPa
Tensile strength	500-700 MPa
Modulus of elasticity	200 MPa

The chamber has been designed to not overcome 100MPa as a safe criterion. The final results are summarized in the Table 3:

Table. 3. Vacuum chamber FEA Results

Characteristic	***Value***
Maximum stress1	110,6 MPa
Wall deformation	0,143 mm
Viewport axis deviation	0,34 mrad

Figure 3.a. Figure 3.b. and Figure 4.a. Figure 4.b. show the maximum stress location and deformations. The maximum deformation of the top cover is about 0,87 mm with 96 MPa of maximum stress.

[1] Von misses equivalent stress

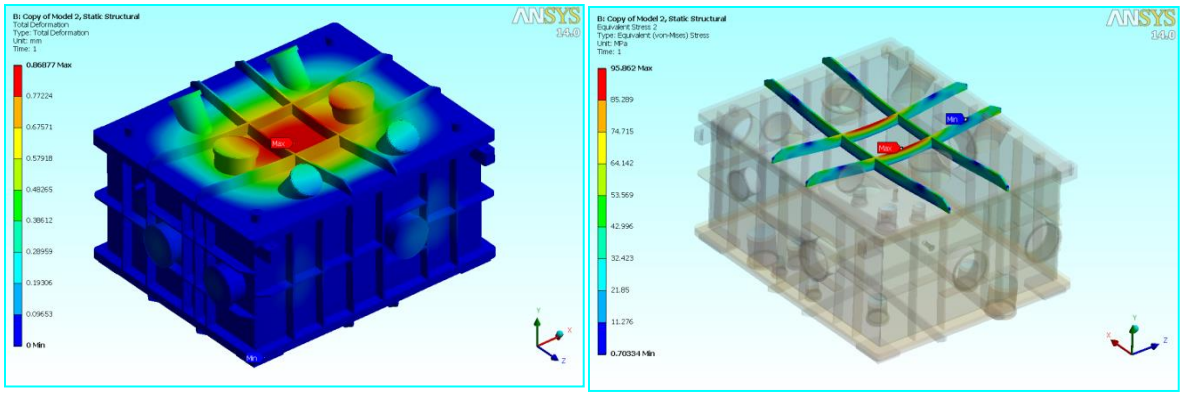

Fig. 3. a. Vacuum chamber top cap deformation b. Vacuum chamber top cover stress

The maximum deformation and stress on the lateral wall are 0,143 mm and 107 MPa respectively.

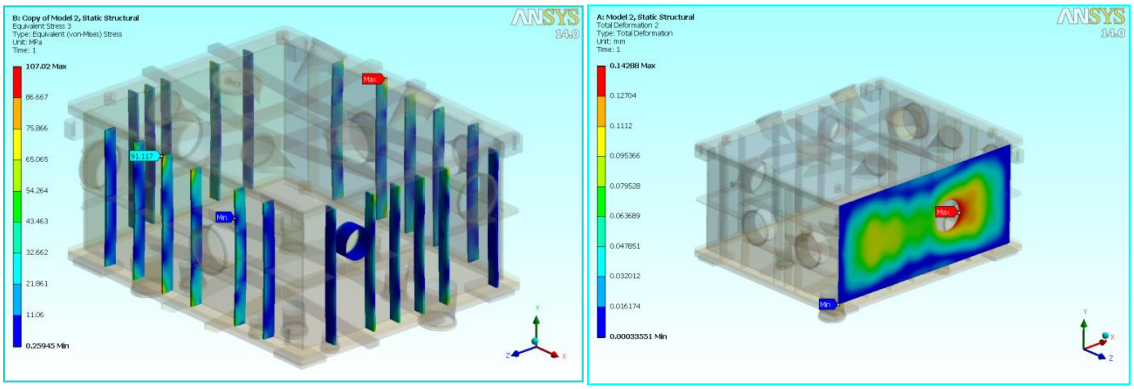

Fig. 4. : a. Vacuum chamber lateral walls stress. b. Vacuum chamber lateral walls deformation

The chamber is expected to be in commissioning at a provisional location, thus the epoxy layer, which glues the base plate to guarantee an accurate flatness between the structure and the ground could not be executed until the placement at the final location. Consequently, it was necessary to study the different possible behaviors of the complete system under various cases in order to have a clear view of the expected results.

The natural frequency modes were calculated for the chamber with FEA. Resonance calculations were made for three assumptions: just lying on regulation screws for the FAT, screwed on the ground for the provisional location and with the final epoxy interface. Figure 5 shows the first resonance modes for the first and third conditions and Table 4 summarizes the first modes:

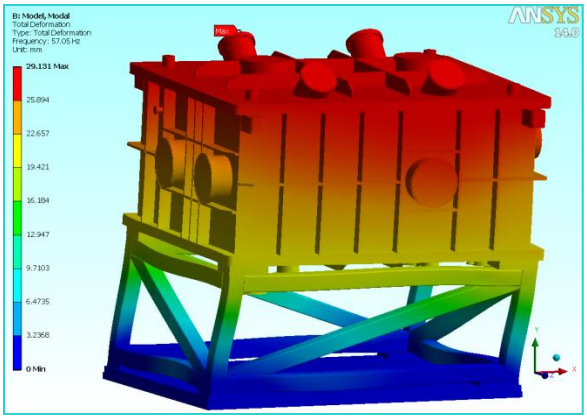

Fig. 5. : Vacuum chamber first resonance mode.

The first column corresponds to the expected results at the final location with the base plates glued with epoxy to the ground. The second column shows the results for FAT solution by leveling without fixing with screws the base plate which will be the condition during FAT. With this calculation we can trust the model validity.

Table. 4. Vacuum chamber calculated resonance modes

Mode	***Epoxy***	***Lying***
1st Mode	57 Hz	1,9 Hz
2nd Mode	62 Hz	31 Hz
3rd Mode	92 Hz	47 Hz

3. 2. Vacuum system

The vacuum system design depends mainly on the pump position and pumping speed. For proper conductance and free flowing path from the pump to the optical equipment, the optimal position would be to be on the top cover of the chamber. Unfortunately this weight on the top will make unstable the opening of the chamber when lifting it by the crane. Furthermore, it would increase severely the level arm in term of vibration excitation. A very compact option is to place the pumps at the bottom cover ports under the chamber. Therefore the pump will be between the granite and the chamber support structure. This will lead to a lower conductance on the optics volume as the breadboard. This will lead to a lower conductance on the volume as the breadboard is partially blocking the flow path between the sensible optical area and the pump. Thus the next step is to dimension properly the pumping speed and the number of pumps.

As a first rough approach analytical vacuum calculations where done with the pumps under the chamber taken in to account the port conductivity and the breadboard impedance with a 400l/s turbo pump. The vacuum level is due the contribution of the degasification of the walls as well as the leak rate on the FKM elastomeric seals.

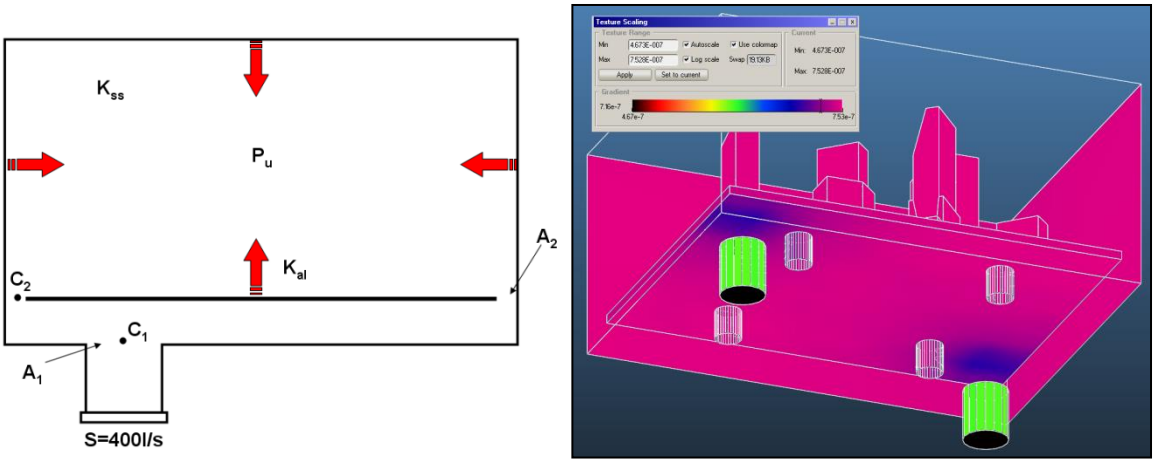

Fig. 6. : a. Vacuum model. b. Moldflow+ simulation.

With the punctual conductivity Equation 1 placed in series the pump port and the breadboard and an estimated value for each material surfaces degasification, the expected vacuum level is calculated as following:

Punctual conductivity:

$$C = 3{,}64\sqrt{\frac{T}{M}A} \tag{1}$$

Where:

- C is conductivity [l/s]
- T is temperature [K]
- M is molecular weight [g/mole]
- A is aperture area [cm2]

Then the effective pumping speed is determined by the expressions Equation 2:

$$\frac{1}{S_{effective}} = \frac{1}{C} + \frac{1}{S} \tag{2}$$

Where S is the pump speed.

In this case is expected to place a single 400 l/s turbo pump. A second spare port is included in the chamber to have room for improvement if were necessary. In order to not increase the chamber price it is considered a mechanically polished inner surfaces with which corresponds to an outgassing about $2{,}27 \cdot 10^{-9}$mbar·l/s·cm^2.

With this the ultimate pressure expected in the chamber could be determined by the expression:

$$P_u = \frac{Q_u}{S_{effective}} \quad (3)$$

Where Qu is the system outgassing.

Then the ultimate pressure at the inside the chamber at the optical elements level volume is $7{,}21 \cdot 10^{-7}$ mbar taken into account that the main pressure contribution at this range is water. This value is under the stipulated specifications.
This is just a preliminary calculation for proper conceptual design dimensioning. Further detailed simulation were done with Moldflow +. Considering the same values applied in the analytical calculation the result is the following:

This is a maximum of $7{,}5 \cdot 10^{-7}$mbar. This result is one order of magnitude less than minimum specified and half of the desired one. This confirms the proper vacuum level at the sensible height plane, confirming that the position of the pump under the chamber is feasible. It also gives a good criterion to place the vacuum sensor just slightly above the lenses holders, as the vacuum at that height is slightly worst, giving us a conservative data. Vacuum calculation available software does not give transient calculations, so the pumping down time is calculated analytically applying Equation 4 (Pfeiffer Vacuum GmbH, 2013) (Bachmann) for each vacuum regime:

$$t = \frac{V}{S_{effective}} \ln\left(\frac{P_i}{P_f}\right) \quad (4)$$

Where:

- V is volume [l]
- S is effective pumping speed [l/s]
- Pi is initial pressure [mbar]
- Pf is final pressure [mbar]

Figure 8 shows the graphic for the calculations considering different input conditions, trying to find a conservative approximation for all surfaces especially for the optical equipment's:

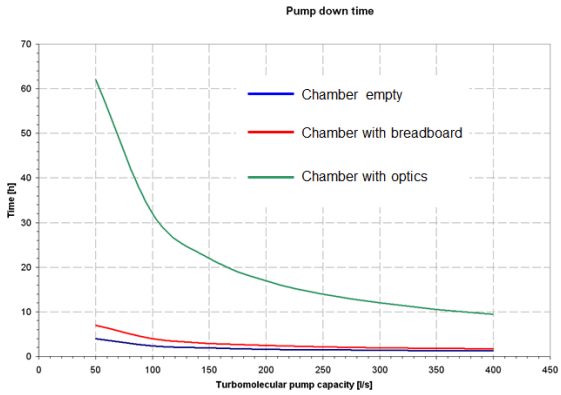

Fig. 8. : Pumping time.

For red and blue trend lines, vacuum chamber is considered empty with no breadboard or optical elements inside. This assumption gives figures for chamber tests moment when the optical elements were not available. The green one corresponds to the approximation with the operational configuration. With this basic calculation it is possible to foresee an enough short evacuation time down to 10^{-6} mbar with just ten hours. This would be the specified speed to have a comfortable intervention and operation of the facility.
Finally and In order to have a friendly access to the optical mounts, the chamber is designed in three parts: a rectangular main single body opened on the bottom as well on the top and sealed by means big rectangular covers. This conception allows lifting up the chamber body, with the top cap mounted on it. This makes possible a free access to the breadboard and optical mounts interventions while leaving the bottom cap on the equipment. Figure 9 shows a simulation of the chamber opening:

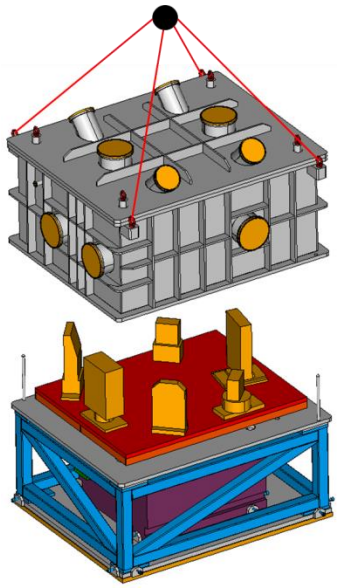

Fig. 9. : Chamber operational opening.

3. 3. Breadboard design & leveling kinematical mount

The basic design of the breadboard is a kinematical mount. It consists of four feet where there are kinematical joints plus one extra flat contact. These joints are supported with four columns which are attached to the big base reference made of granite. Figure 10.a. shows the detailed design of the subsystem:

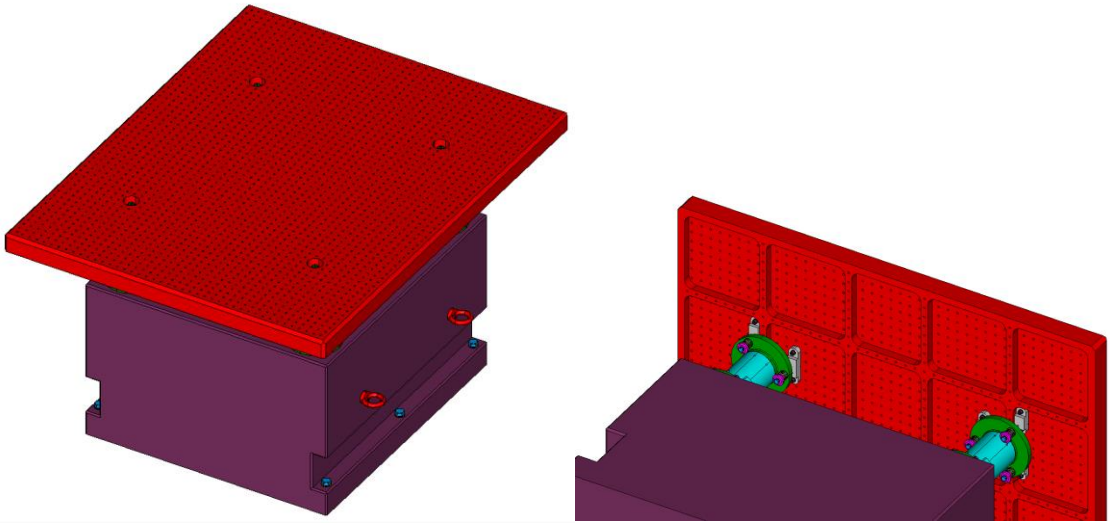

Fig. 10. : a. Optics Breadboard. b. Kinematical link columns.

The kinematical mount includes the three classic contacts (cone, V slot and plane) and an extra plane contact. The latter avoids leaving long free winds that may reduce the stiffness. At the same time, it prevents from roll natural frequency mode on the breadboard. Figure 10.b. shows a bottom view oriented of a kinematical link column:

Despite the weight, a kinematical mount is based in just lying on the dry contacts. In order to increase the stiffness and consequently the stability of the optical base a spring preloaded system which allows the leveling adjustment is proposed. This spring preloaded kinematical mount includes fine pitch regulation screws hold by means a backslash free counter fixation nut. See Figure 11 where the preloaded kinematical mechanism in detail:

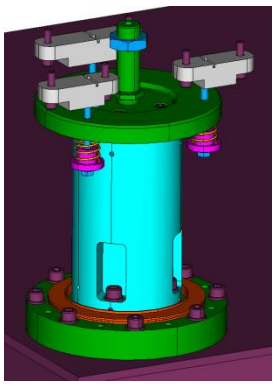

Fig. 11. Kinematical preloaded columns detail.

The preload is based on compressions spring squeezing at its both extremes spherical washers which allows the leveling angular relieving. The kinematical links are attached to the four columns through the bottom chamber cover. Hydro formed bellow surrounding the columns are both connected to a blanking flange rigidly screwed to the granite. This decoupling isolates the breadboard from the chamber's heavy mass. Otherwise, it would induce big vibrations amplitudes on the system. This granite stone is also rigidly fixed to the ground. A steel base plate glued with an intermediate epoxy in the same way as the chamber frame. Both plates are independent so no vibration is transmitted between them. The design criterion for the columns positioning is the minimization of the breadboard deformations induced by its own weight and the optical instrumentation payload, besides the vibration stability. Ensuring these premises, the breadboard will be a flat reference for the system. FEA calculations studying the free vibration behavior were done. Figure 12. a. shows the breadboard deformation and first resonance mode.

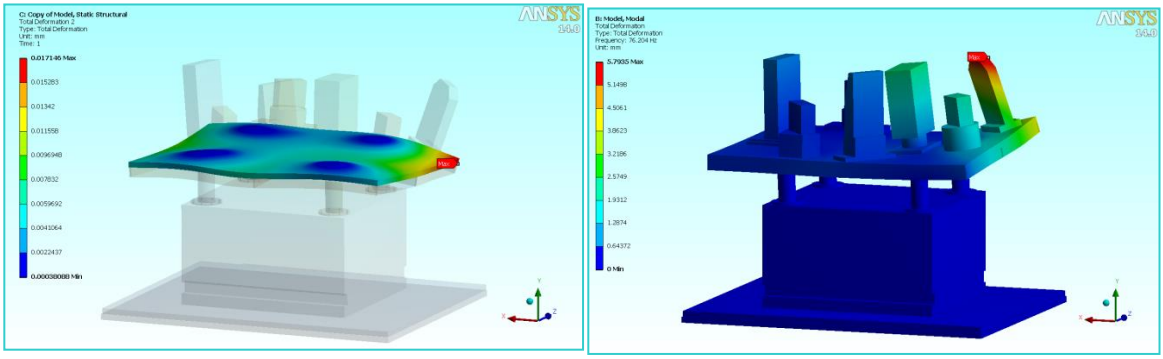

Fig. 12. : a. Breadboard deformation. b. Breadboard first resonance mode.

Maximum expected deformation value was 0,017 mm.

In the same manner as the chamber calculations, three ground fixation cases are simulated for the FAT (factory acceptance test) and the permanent location: a provisional placement lying on regulation screws, a screwed fixation to the ground and the final set up with the epoxy layer interface between the steel base plate and the ground. Table 5 summarizes the results:

Table. 5. Breadboard calculated resonance modes

Mode	***Epoxy***	***Lying***
1st Mode	45 Hz	0.56Hz
2nd Mode	58 Hz	34 Hz
3rd Mode	69 Hz	42 Hz

The kinematical mount contacts are simulated by no separation boundary conditions. This maintains the contact but allowing sliding in all cases. The 3D model geometry simulates the kinematical mounts restrictions. These calculations gave the criterion to optimize the diameter of the columns. The results confirms that despite the kinematical mount is not conceptually very rigid, a proper dimensioning will lead to the desired stability. This ensures that the first resonance modes are away from environmental excitation avoiding amplification of these sources.

3. 4. Vacuum windows

The holder for the vacuum windows consists of clamping the borosilicate glass between two FKM elastomeric O-rings, in vacuum and air side respectively. Two customized ISO-K 200 flanges grasp the glass against the O-rings. A slight pre-load is applied to avoid unclamping during manipulation or venting of the chamber, so no loss of contact between the O-ring and the glass occurs on the air side when it's under vacuum atmospheric pressure load. This mounting avoids holding stresses of a rigid clamp. In addition the BK7 glass deformation is radially symmetrical under vacuum pressure. This solution adopted is also easy installing and self-centering, making the set up really straightforward without special tools and quick in-situ replacements. Figure 13. a. shows a cross section of this design:

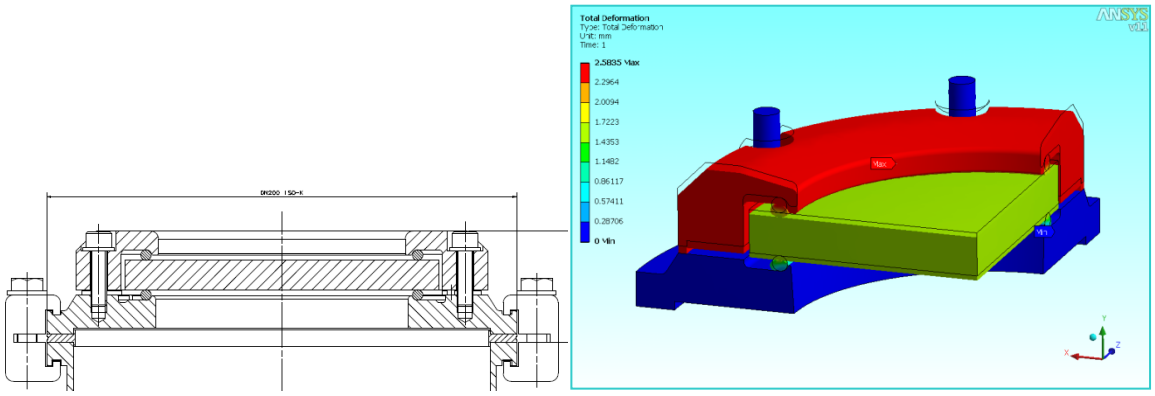

Fig. 13. : a. Viewport cross section. b. Viewport holder simulation.

FEA calculations were also made for the viewport model applying special material characteristics to simulate the elastomeric behavior of the rings. Three assumptions were followed: first do not collapse the vacuum sealing O-Ring; second do not lose the contact with Viton ring at the vacuum side and finally does not reach the stress limit for the borosilicate.

During its mounting at atmospheric pressure, both rings are compressed symmetrically 1,25 mm. When vacuum force is applied, the air side ring still remains with 0,8 mm compressed. The maximum stress introduced under the vacuum load on the BK7 glass was calculated. Little literature was found about the material characteristics (Andrew Bachmann, 2001).

Table. 6. Window material properties

Material	***Yield strength***	***Tensile strength***	***Modulus of elasticity***
AISI-304	190 MPa	500-700 MPa	200 MPa
BK7	-	6.9 MPa	81.0 GPa

Figure 14. a. shows the stress distribution on the glass. The Y axis of the calculated portion is used to constrain symmetrically and fixing the model allowing axial deformation. From a conservative point of view, the stress worst scene has been studied. Sliding contacts constrains has been applied on the glass holders permitting the completely free deformation of the glass in the Y axis direction.

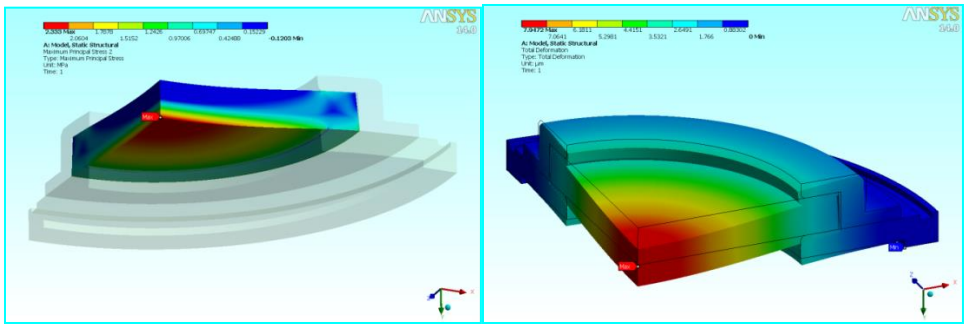

Fig. 14. : a. BK7 glass stress simulation. b. Window deformation.

The maximum Von Misses equivalent stress is 2,33 MPa. The maximum tensile stress (Andrew Bachmann, 2001) allowed for BK7 is 6,9 MPa so there is a 2,5 safety factor. Figure 14. b. shows the deformation map of the window:

The cross section profile:

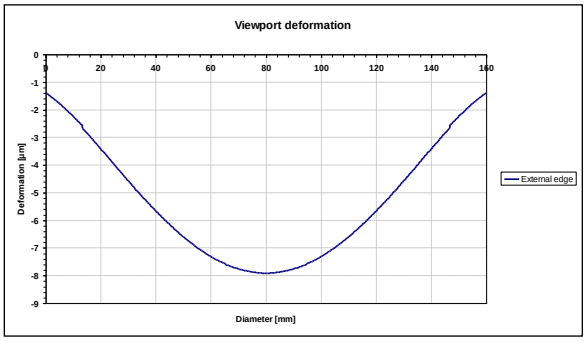

Fig. 15. : Window deformation profile.

The highest value at the center zone was 7,95 µm, which is perfectly acceptable. Simulation results are summarized on Table 7. The maximum acceptable stress for the glass is not specified by the material supplier and even in the literature is difficult by the BK7 it.

Table. 7. window design results

Characteristic	***Value***
Maximum stress[2]	2,33 MPa
Window deformation	7,95 µm
Viewport axis deviation	0 mrad
In-Vacuum O-Ring compression	2,5 mm

[2] Von misses equivalent stress

Despite these good results regarding the deformation and deviation of the port, a hydro formed bellow with three support/regulation rods with a sensibility of 0,29 mrad was introduced. The negligible axis deviation coming from the chamber and the zero deviation of the window ensures a nominal positioning of the bellow in the relaxed point. Therefore, complete bellow stroke is available for the operation of the laser beam and window alignment.

4. Manufacturing/construction

Despite the high demanding design specifications, the manufacturing went to a quite conventional outsourcing. The adjudication is organized in different sets depending on the characteristics of the production process: The vacuum chamber, the granite, steel frame and out vacuum conventional parts, out vacuum base plates, in vacuum mechanical parts, and the breadboard which is also in-vacuum. Just few special details the kinematical mount contacts parts are made with AISI-420B tempered and stress relieve annealing for full compliance contact.

5. Quality assurance

The Factory Acceptance Tests were done at ALBA premises. Not all design results were tested but few sample measurements were done.

- A prototype of the view port
- Vacuum chamber wall deformation
- Vacuum level and pumping down time
- Vibrations without epoxy glue.

5. 1. Viewport test

Figure 16 shows an in-house made prototype manufactured for testing, as there is no previous experience with borosilicate glass:

Fig. 16. : Window prototype.

Basic vacuum tests were performed to the window with following results:

Table. 8. Viewport tests

Characteristic	***Performance***
Vacuum level	$5{,}7 \cdot 10^{-7}$ mbar
Leak background	10^{-9} mbar·l/s
Glass vacuum displacement	0,2 mm

The deformations were measured by means micrometric indicators.

5. 2. Chamber tests

Special accessible points on the chamber were chosen where to acquire vacuum mechanical deformations. Figure 17 shows the expected results in these selected areas corresponding to the laser input port and the bottom cover:

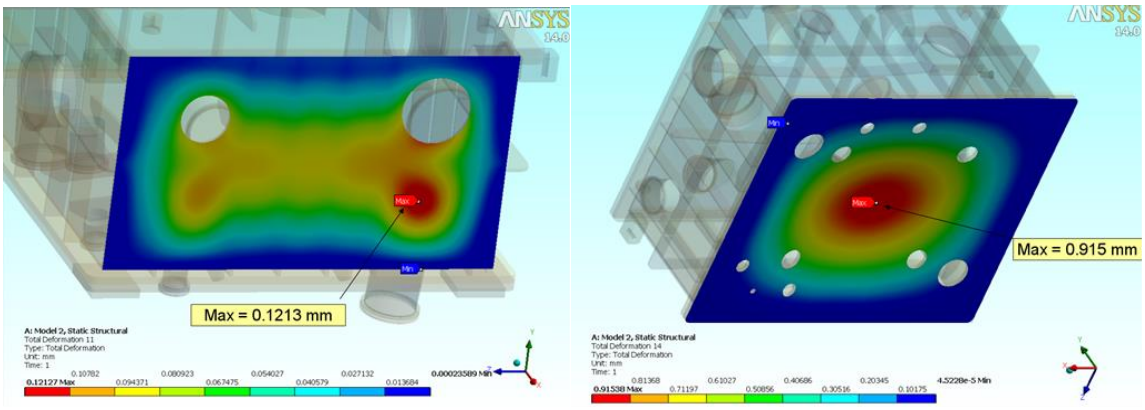

Fig. 17. : a. Test reference point. b. Test reference point

Figure 17. b. shows the selected zone for the bottom cover and Table 9 shows the summary for the expected values and final tested figures:

Table. 9. Chamber tests

Characteristic	***Expected, FEA***	***Tested***
Wall	0,12 mm	0,13 mm
Bottom cover	0,814 to 0,712mm	0,760 mm

5. 3. Vacuum tests

Vacuum tests were done using a turbo pump of 600 l/s capacity, obtaining the following pressure values:

- Vacuum after 12h pumping: $1{,}1 \cdot 10^{-6}$ mbar
- Vacuum after 24h pumping. $9{,}0 \cdot 10^{-7}$ mbar
- Long term: $3{,}6 \cdot 10^{-7}$ mbar.

The specified was $5 \cdot 10^{-6}$mbar after first 10 h of pumping. Figure 18 shows the test evolution along time:

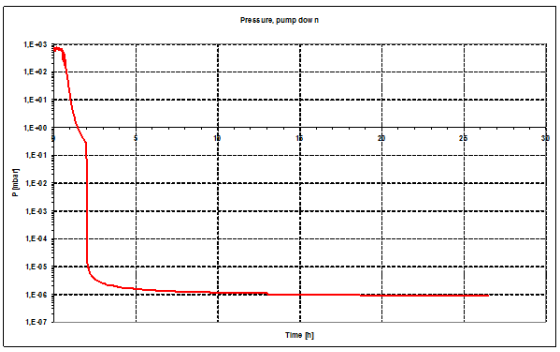

Fig. 18. : Vacuum vs time.

Table. 10. Chamber tests

Characteristic	***Calculated***	***Tested***
Ultimate pressure	7,5·10-7mbar	3,6·10-7mbar
Pumping time up to 5·10-6mbar	<10h	2,5 h
Leak detection	2,27·10-9 mbar·l/s·cm2	10-9 mbar·l/s

5. 4. Stability tests

Vibration test on the breadboard were done with Laser interferometer ML10. Some weight were placed on the breadboard to simulate optics payloads. Figure 19 shows the vibration spectrum in µm.

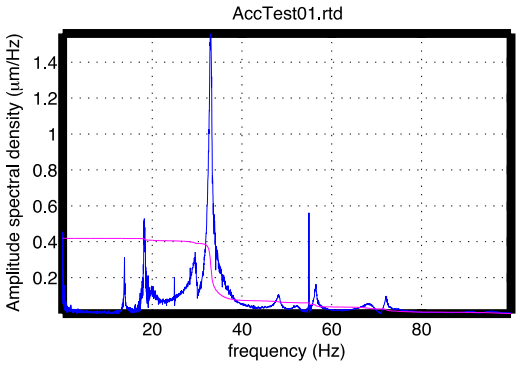

Fig. 19. : Vibration Spectrum.

For the FAT conditions, the fixation of the breadboard to the ground consists only of laying on the screws with no epoxy layer. There is a clear resonance mode at 33 Hz which corresponds exactly with the second calculated resonance see Table 6. The first expected mode was at 25 Hz and this also validates the epoxy modelling not tested yet as seems the simulation it is in the safe side. The root mean squared RMS displacement amplitude measured was 52 nm. This value is quite lower than the micron requested. It is worth noticing that the FAT was done at ALBA workshop, which is a quite vibration excitation active area regarding the ground behavior. The fact confirms again that the results can be considered in a very conservative side.

Table 11 contains the stability results for the breadboard tests:

Table. 11. Stability test

Characteristic	*Calculated*	*Tested*
1st mode	0.56Hz	-
2nd mode	34 Hz	33 Hz
3rd mode	42 Hz	-
Amplitude	< 1 µm	52 nm

4. Conclusion

In conclusion, a new overall design for a laser compressor, different from the conventional laser facilities ones, has been successfully implemented. The conceptual and detailed design of the vacuum chamber, breadboard with kinematical mount, frame structure and laser viewports were validated using FEA calculations simulating real field conditions. Manufacturing and mounting process was supervised in order to accomplish all the technical requirements. Final quality assurance stage corroborated better results than the expected values calculated by FEA. All dimensional checking, vacuum testing and vibration analysis were carried out at ALBA facilities. The technical experience acquired during the construction and commissioning of ALBA synchrotron facility could be well adapted to other kind of scientific applications properly converted.

Acknowledgements

Authors wish to acknowledge all mostly involved in the design and construction: Marta Llonch (alignment group), Josep Nicolas (Optics group), Jose Ferrer (technicians head), David Calderón (Technician), Karim Maimouni (Technician), Lluis Gines (vacuum technician), Jordi Navarro (vacuum technician).

We acknowledge support from LaserLab-Europe (Grant No. EU-FP7 284464).

References

Andrew Bachmann, D. J. (2001). CONTROLLING STRESS IN BONDED OPTICS. Connecticut: DYMAX Corporation.

Pfeiffer Vacuum GmbH. (2013). Vacuum Technology Book Volume II: Know-How book. Asslar: Pfeiffer Vacuum GmbH.